Evolution of 2-DE methodology

SDS-PAGE Gel size:

- This “O’Farrell” techniques has been used for 20 years without major modification.
- 20 x 20 cm have become a standard for 2-DE.
- Assumption: 100 bands can be resolved by 20 cm long 1-DE.
- Therefore, 20 x 20 cm gel can resolved 100 x 100 = 10,000 proteins, in theory.

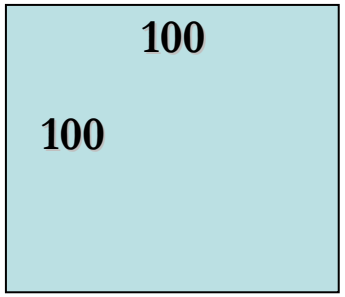

2-D PAGE according to Klose and O'Farrell

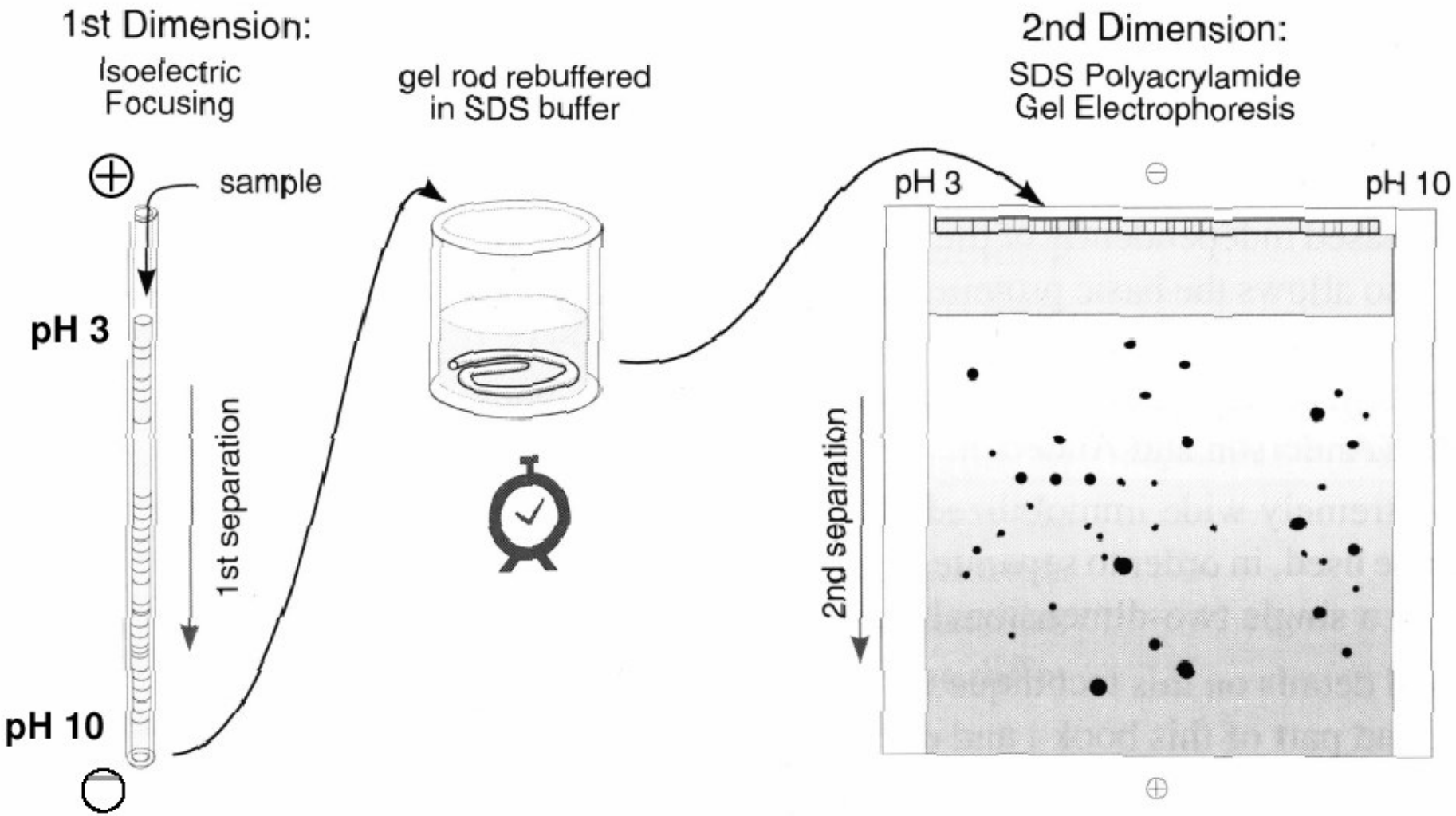

pI Gradients Using Carrier Ampholytes – O'Farrell

- Small amphoteric molecules which have high buffering capacities near their pI
- Generally a poorly defined mixture of molecules
  - Poor batch to batch reproducibility
- Align themselves in the electric field according to their pI.
- pI gradients are unstable and tend to drift toward the cathode over time.
- Difficult to work with soft acrylamide tube gels.
  - Operator dependent

Separation of *E. coli* Proteins in 1975

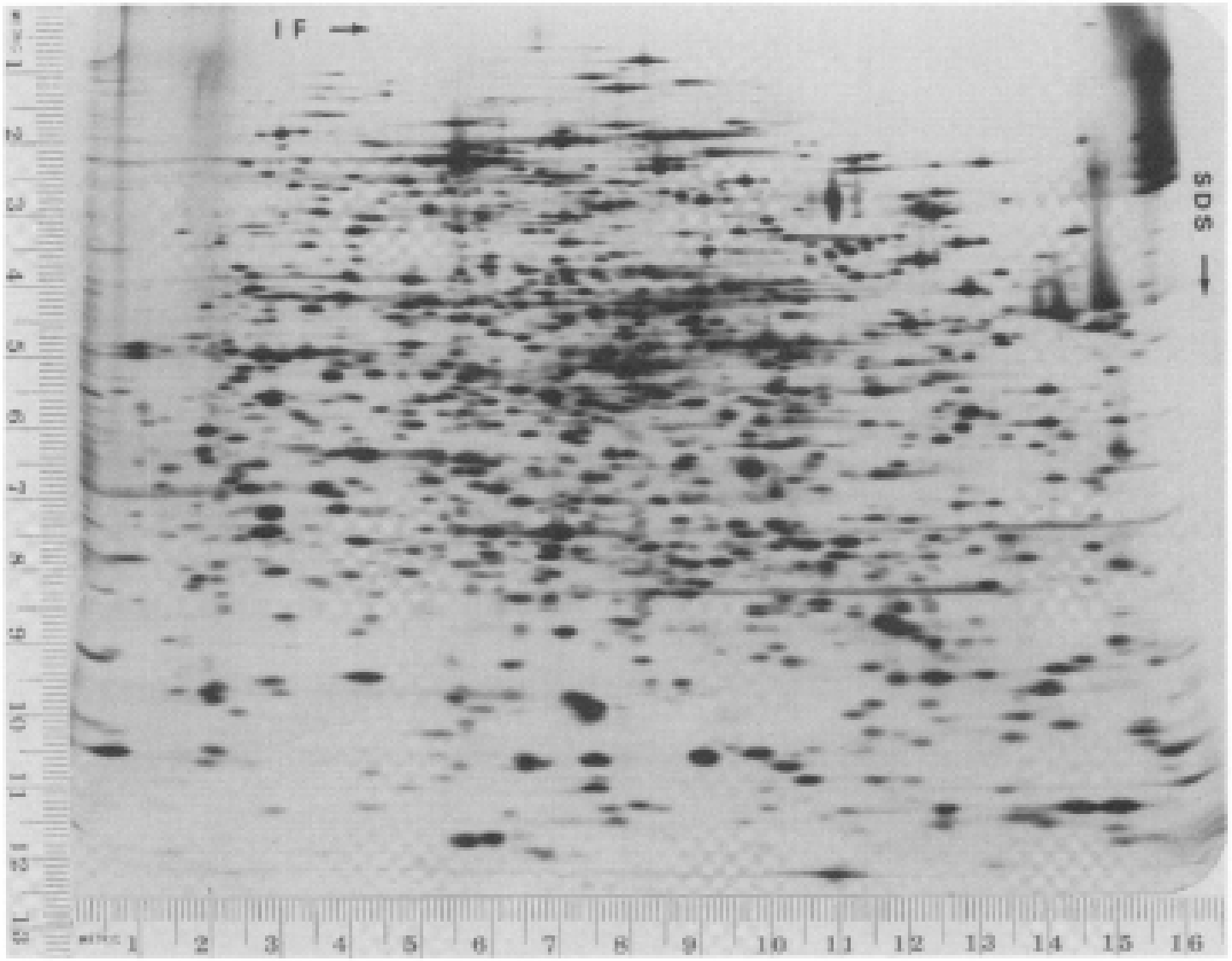

1D to 2D Comparison

2D-PAGE according to Görg *et al.*

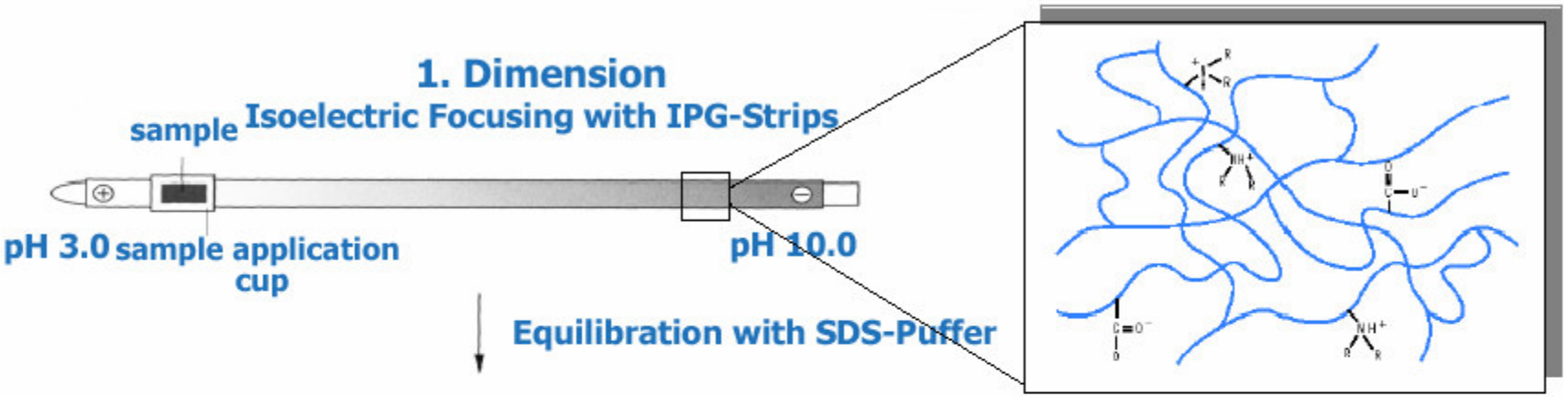

Immobilised pH gradients, IPG

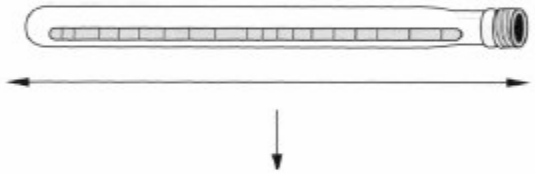

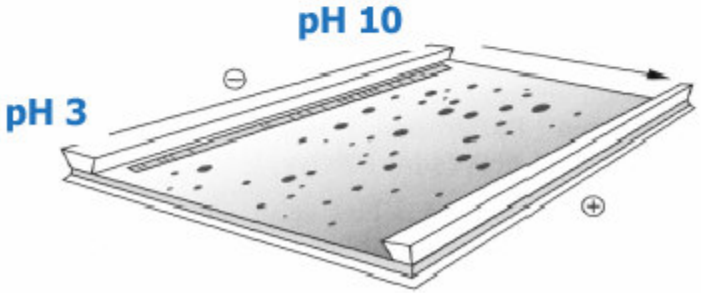

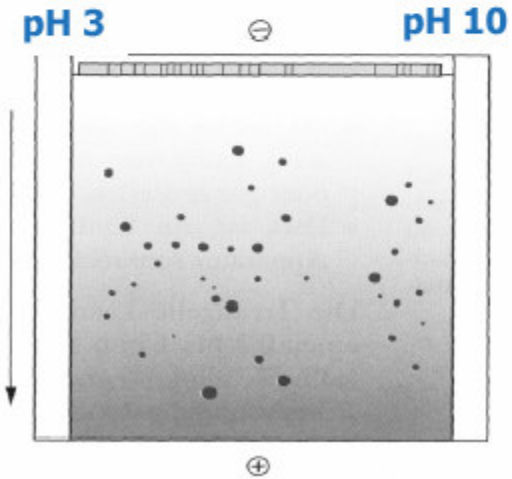

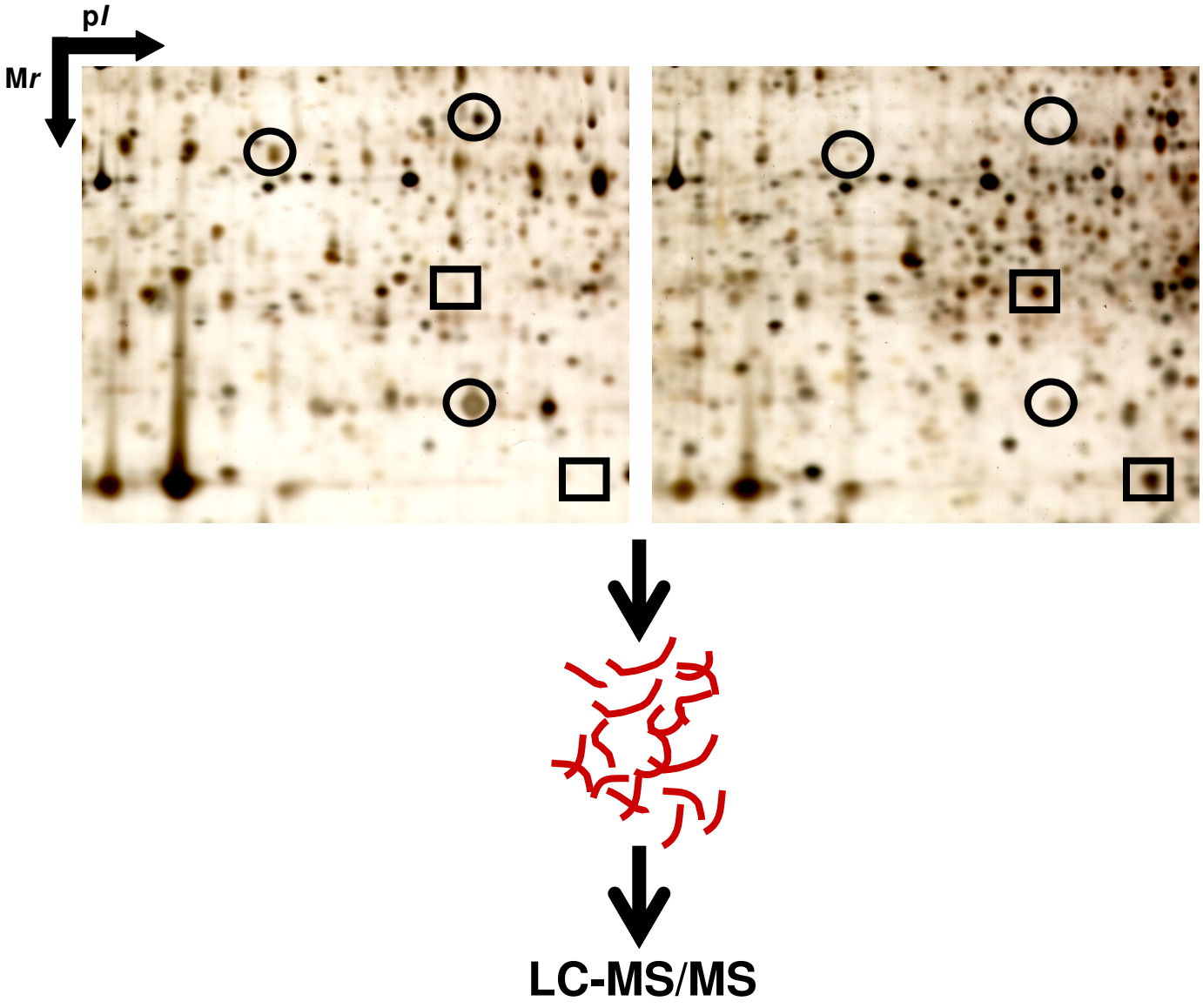
pI
Mr
LC-MS/MS

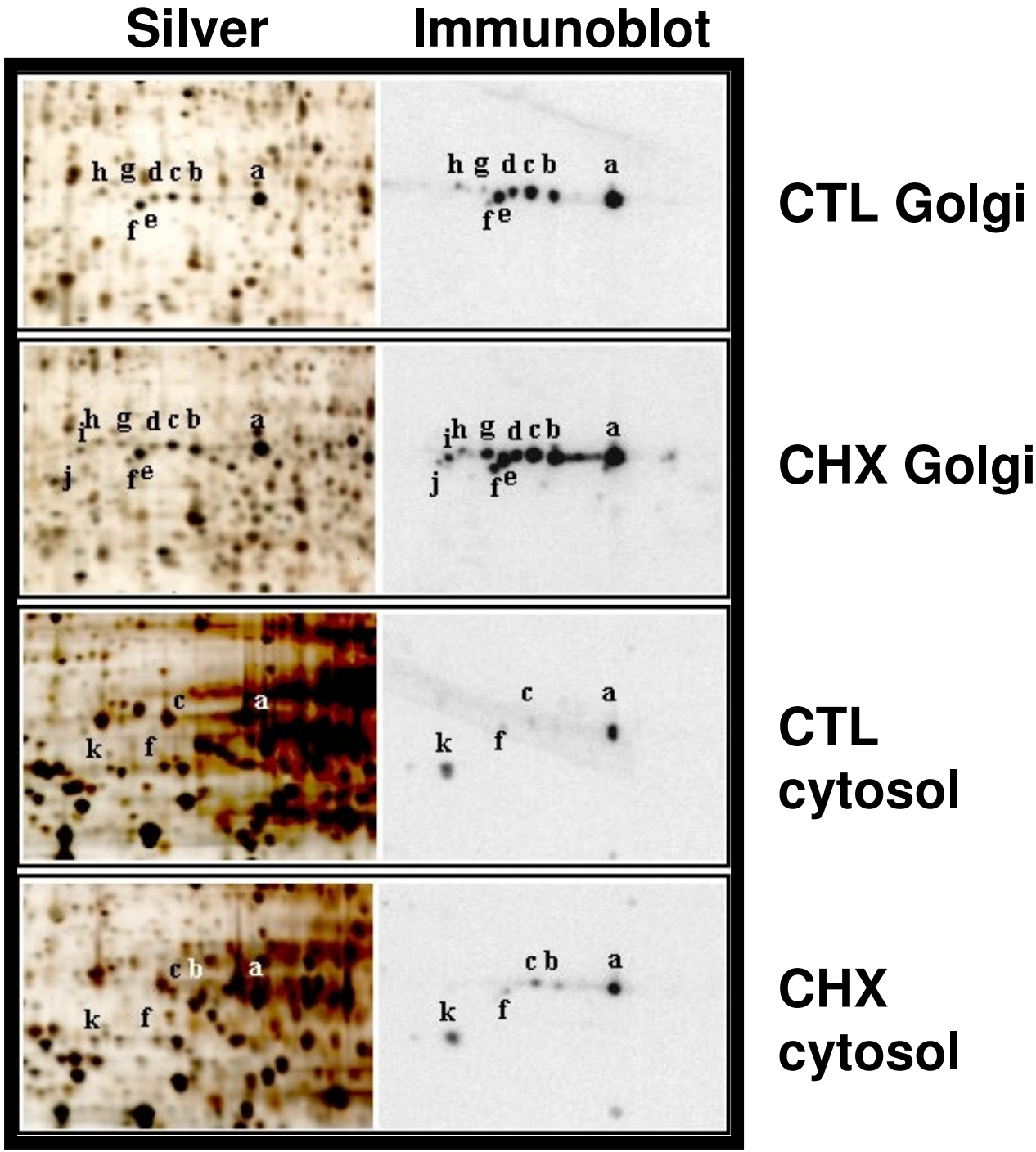
Silver
Immunoblot
h g d c b a
f e
h g d c b a
f e
CTL Golgi
i h g d c b a
j f e
i h g d c b a
j f e
CHX Golgi
c a
k f
c a
k f
CTL
cytosol
c b a
k f
c b a
k f
CHX
cytosol

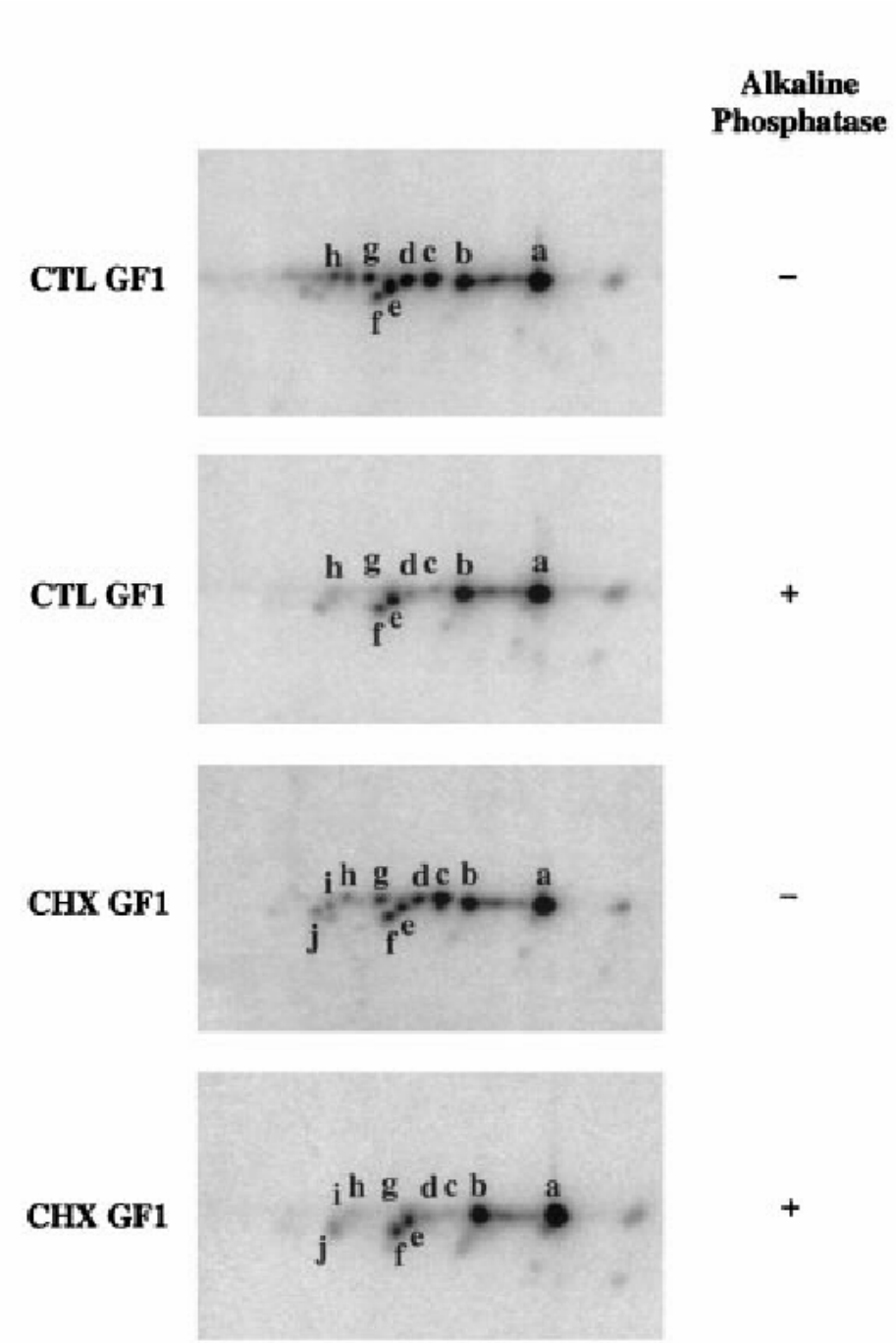
Alkaline Phosphatase
CTL GF1
h g d c b a
f e
–
CTL GF1
h g d c b a
f e
+
CHX GF1
i h g d c b a
j f e
–
CHX GF1
i h g d c b a
j f e
+

Traditional 2-D electrophoresis

Four different samples run on four different gels.

The abundance of this particular protein spot appears to be increasing in samples 3 and 4. Is this increase due to system variation or induced biological change?

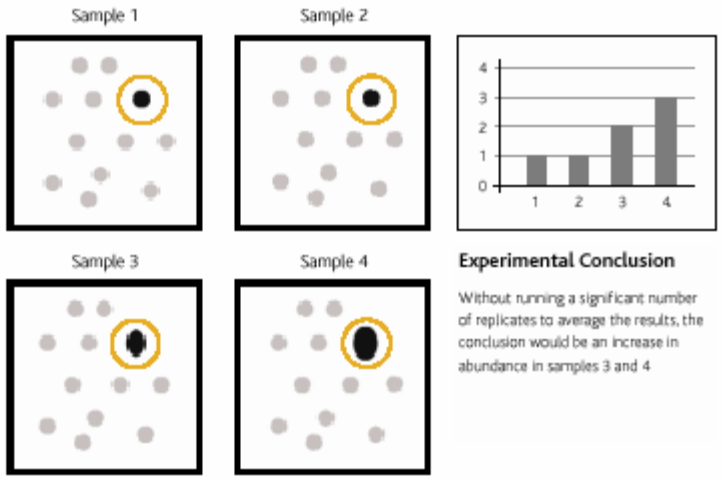

Experimental Conclusion

Without running a significant number of replicates to average the results, the conclusion would be an increase in abundance in samples 3 and 4

Ettan DIGE using an internal standard

Four different samples, plus one internal standard, on two different gels.

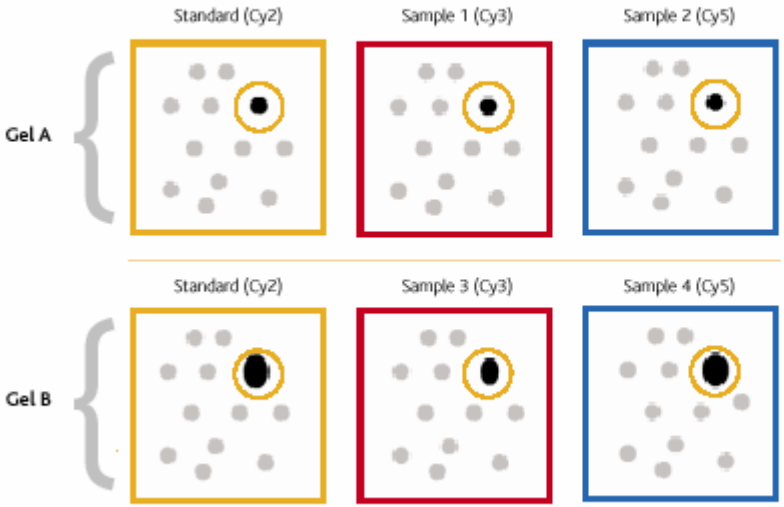

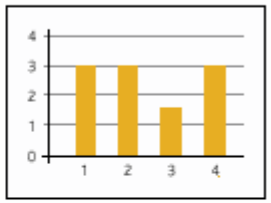

Experimental Conclusion

The same internal standard is run on both gels. The increase in abundance of protein in gel B, as shown by the increase in the internal standard, is due to gel-to-gel variation. When the internal standard is normalized between gels A and B the conclusion is the abundance of protein in sample 3 has actually decreased.

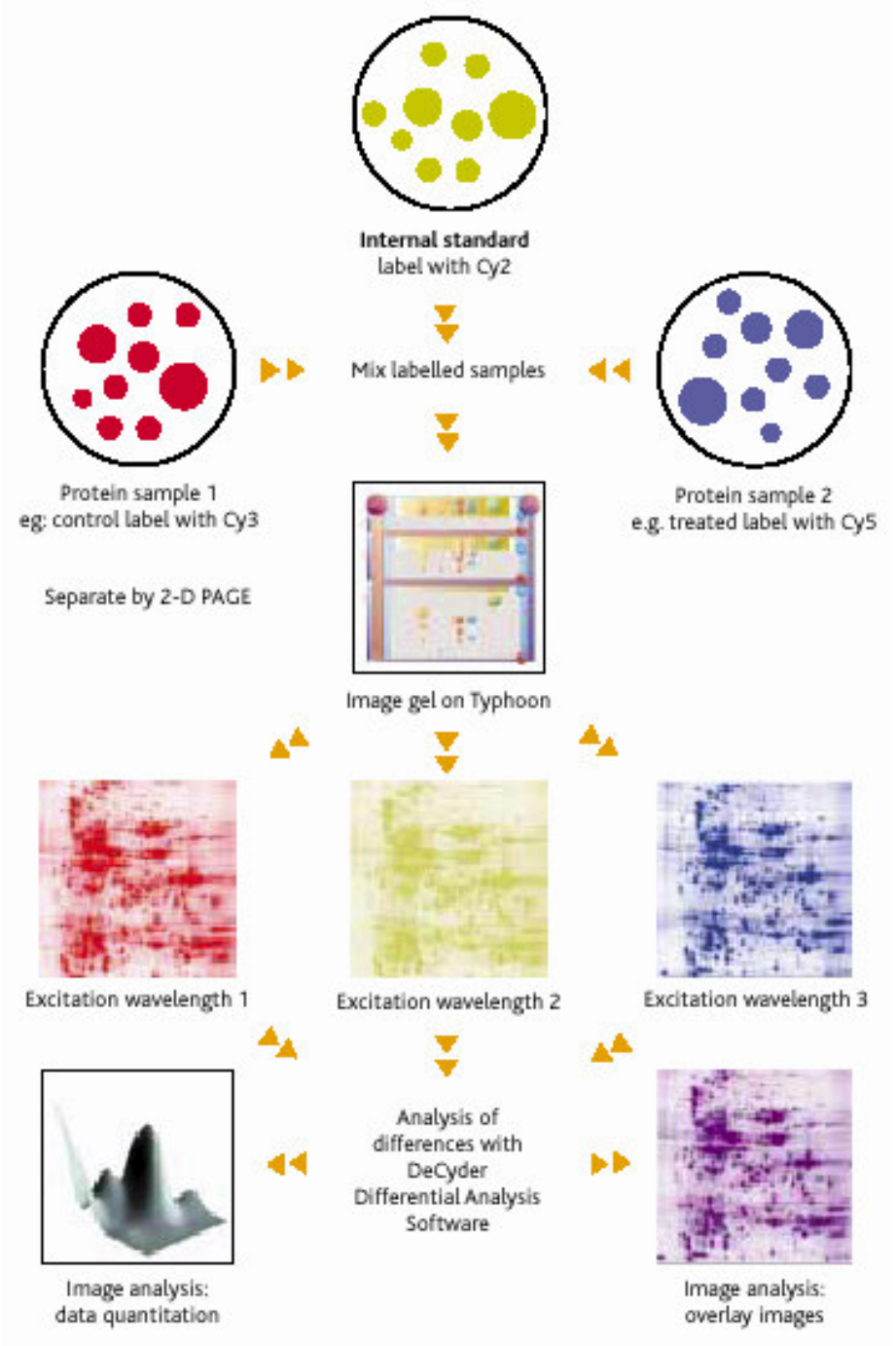

Each CyDye DIGE Fluor minimal dye, when coupled to a protein, will add approximately 500 Da to the mass of the protein. This mass shift does not effect the pattern visible on a 2-D gel.

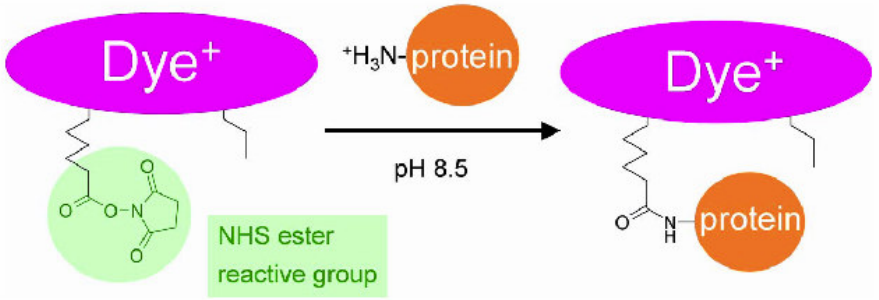

Fig 1-2. Schematic of the minimal labelling reaction. CyDye DIGE Fluor minimal dye containing NHS ester active group covalently binds to the lysine residue of a protein via an amide linkage.

Correlation between Protein and mRNA Abundance in Yeast

STEVEN P. GYGI, YVAN ROCHON, B. ROBERT FRANZA, AND RUEDI AEBERSOLD*

Department of Molecular Biotechnology, University of Washington, Seattle, Washington 98195-7730

Received 5 October 1998/Returned for modification 11 November 1998/Accepted 2 December 1998

We have determined the relationship between mRNA and protein expression levels for selected genes expressed in the yeast *Saccharomyces cerevisiae* growing at mid-log phase. The proteins contained in total yeast cell lysate were separated by high-resolution two-dimensional (2D) gel electrophoresis. Over 150 protein spots were excised and identified by capillary liquid chromatography-tandem mass spectrometry (LC-MS/MS). Protein spots were quantified by metabolic labeling and scintillation counting. Corresponding mRNA levels were calculated from serial analysis of gene expression (SAGE) frequency tables (V. E. Velculescu, L. Zhang, W. Zhou, J. Vogelstein, M. A. Basrai, D. E. Bassett, Jr., P. Hieter, B. Vogelstein, and K. W. Kinzler, Cell 88:243–251, 1997). We found that the correlation between mRNA and protein levels was insufficient to predict protein expression levels from quantitative mRNA data. Indeed, for some genes, while the mRNA levels were of the same value the protein levels varied by more than 20-fold. Conversely, invariant steady-state levels of certain proteins were observed with respective mRNA transcript levels that varied by as much as 30-fold. Another interesting observation is that codon bias is not a predictor of either protein or mRNA levels. Our results clearly delineate the technical boundaries of current approaches for quantitative analysis of protein expression and reveal that simple deduction from mRNA transcript analysis is insufficient.

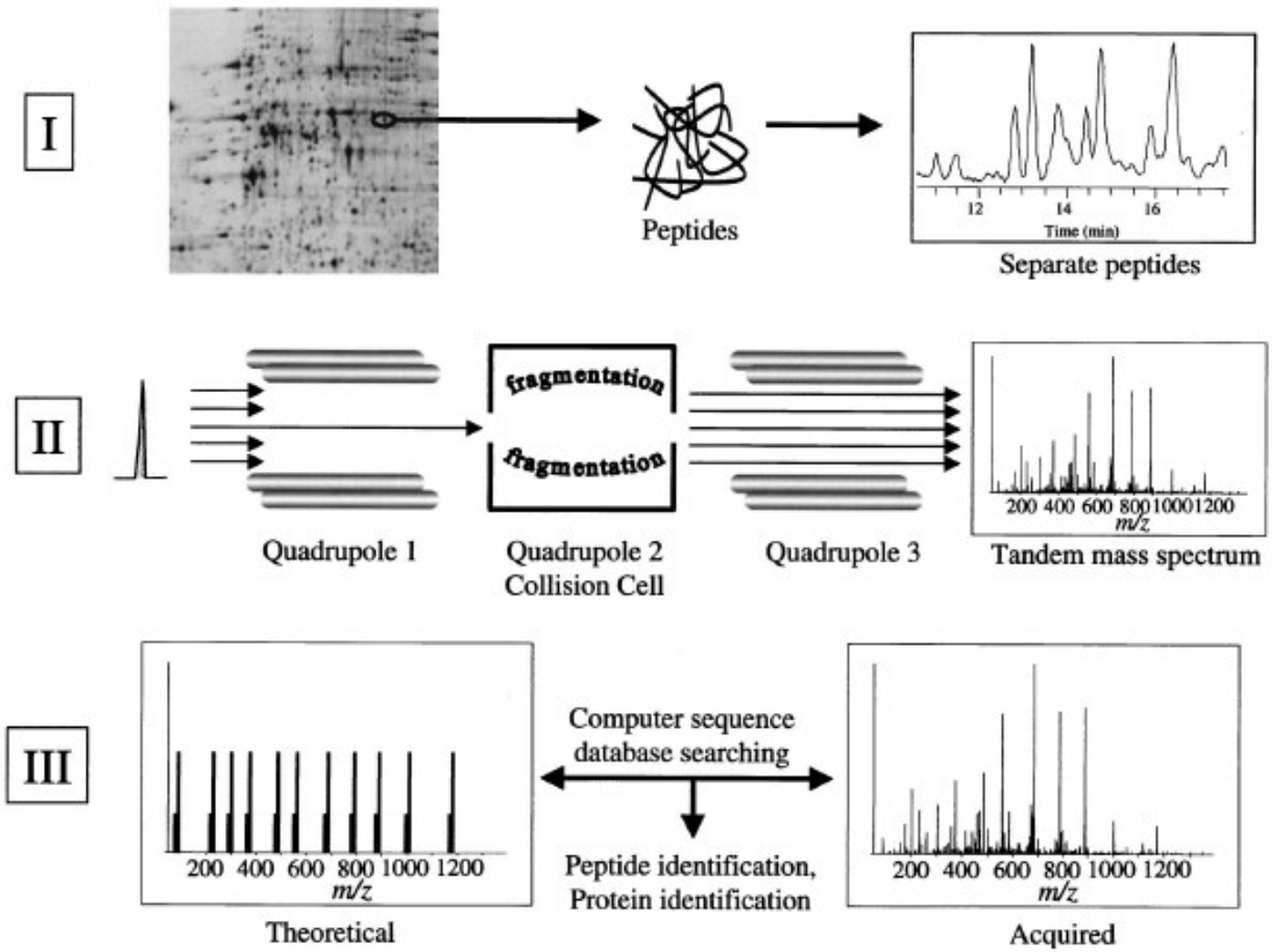

FIG. 1. Schematic illustration of proteome analysis by 2DE and mass spectrometry. In part I, proteins are separated by 2DE, stained spots are excised and subjected to in-gel digestion with trypsin, and the resulting peptides are separated by on-line capillary high-performance liquid chromatography. In part II, a peptide is shown eluting from the column in part I. The peptide is ionized by electrospray ionization and enters the mass spectrometer. The mass of the ionized peptide is detected, and the first quadrupole mass filter allows only the specific mass-to-charge ratio of the selected peptide ion to pass into the collision cell. In the collision cell, the energized, ionized peptides collide with neutral argon gas molecules. Fragmentation of the peptide is essentially random but occurs mainly at the peptide bonds, resulting in smaller peptides of differing lengths (masses). These peptide fragments are detected as a tandem mass (MS/MS) spectrum in the third quadrupole mass filter where two ion series are recorded simultaneously, one each from sequencing inward from the N and C termini of the peptide, respectively. In part III, the MS/MS spectrum from the selected, ionized peptide is compared to predicted tandem mass spectra computer generated from a sequence database. Provided that the peptide sequence exists in the database, the peptide and, by association, the protein from which the peptide was derived can be identified. Unambiguous protein identification is attained in a single analysis because multiple peptides are identified as being derived from the same protein.

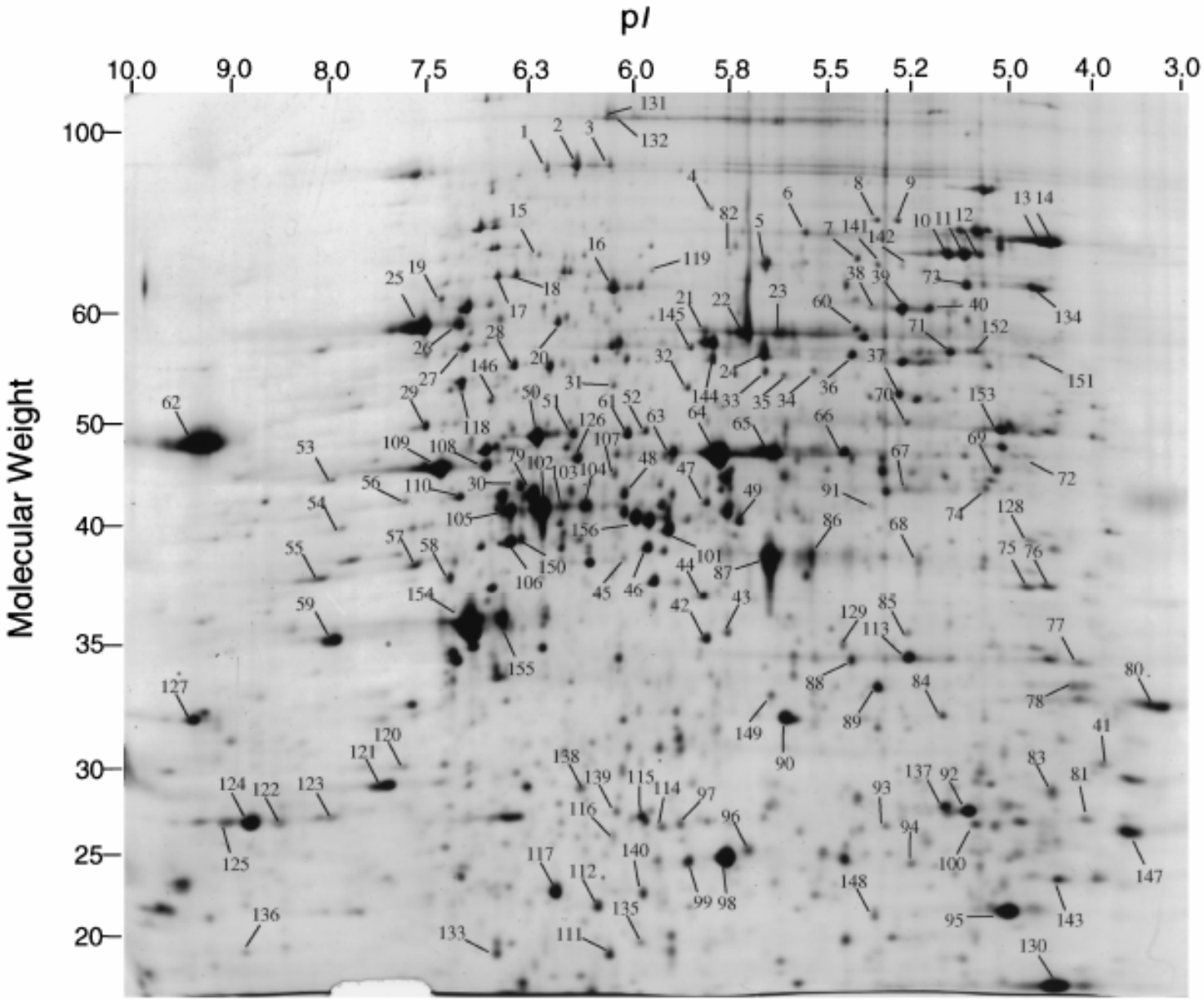

FIG. 2. 2D silver-stained gel of the proteins in yeast total cell lysate. Proteins were separated in the first dimension (horizontal) by isoelectric focusing and then in the second dimension (vertical) by molecular weight sieving. Protein spots (156) were chosen to include the entire range of molecular weights, isoelectric focusing points, and staining intensities. Spots were excised, and the corresponding protein was identified by mass spectrometry and database searching. The spots are labeled on the gel and correspond to the data presented in Table 1. Molecular weights are given in thousands.

TABLE 1. Expressed genes identified from 2D gel in Fig. 2

Mol wt	pI	Spot no.	YPD gene name[a]	Protein abundance (10^3 copies/cell)	mRNA abundance (copies/cell)	Codon bias
17,259	6.75	133	CPR1	15.2	61.7	0.769
18,702	4.80	83	EGD2	20.1	5.2	0.724
18,726	4.44	147	YKL056C	61.2	88.4	0.831
18,978	5.95	135	YER067W	3.7	6.7	0.118
19,108	5.04	130	YLR109W	94.4	9.7	0.680
19,681	9.08	136	ATP7	11.0	NA[b,c]	0.246
20,505	6.07	111	GUK1	16.5	3.7	0.422
21,444	5.25	148	SAR1	5.4	10.4	0.455
21,583	4.98	95	TSA1	110.6	40.1	0.845
22,602	4.30	80	EFB1	66.1	23.8	0.875
23,079	6.29	112	SOD2	12.6	2.2	0.351
23,743	5.44	137	HSP26	NA[d]	0.7	0.434
24,033	5.97	96	ADK1	17.4	16.4	0.656
24,058	4.43	143	YKL117W	29.2	10.4	0.339
24,353	6.30	140	TFS1	8.1	0.7	0.146
24,662	5.85	99	URA5	25.4	6.0	0.359
24,808	6.33	97	GSP1	26.3	5.2	0.735
24,908	8.73	122	RPS5	18.6	NA[c]	0.899
25,081	4.65	81	MRP8	9.3	NA[c]	0.241
25,960	6.06	116	RPE1	5.8	0.7	0.372
26,378	9.55	127	RPS3	96.8	NA[c]	0.863
26,467	5.18	100	VMA4	10.5	3.7	0.427
26,661	5.84	98	TPI1	NA[d]	NA[c]	0.900
27,156	5.56	93	PRE8	6.9	0.7	0.129
27,334	6.13	115	YHR049W	18.4	2.2	0.520
27,472	5.33	92	YNL010W	31.6	3.7	0.421
27,480	8.95	123	GPM1	10.0	169.4	0.902
27,480	8.95	124	GPM1	231.4	169.4	0.902
27,480	8.95	125	GPM1	7.5	169.4	0.902
27,809	5.97	139	HOR2	5.7	0.7	0.381
27,874	4.46	78	YST1	13.6	52.8	0.805
28,595	4.51	41	PUP2	4.4	0.7	0.147
29,156	6.59	114	YMR226C	14.5	2.2	0.283
29,244	8.40	120	DPM1	5.0	11.2	0.362
29,443	5.91	48	PRE4	3.4	3.7	0.162
30,012	6.39	138	PRB1	21.2	1.5	0.449
30,073	4.63	77	BMH1	14.7	28.2	0.454
30,296	7.94	121	OMP2	67.4	41.6	0.499
30,435	6.34	89	GPP1	70.2	11.2	0.703
31,332	5.57	88	ILV6	13.9	3.0	0.402
32,159	5.46	113	IPP1	63.1	3.7	0.752
32,263	6.00	149	HIS1	22.4	4.5	0.232
39,477	5.58	86	FBA1	17.8	183.6	0.935
39,477	5.58	87	FBA1	427.2	183.6	0.935
39,540	6.50	150	HOM2	60.3	4.5	0.592
39,561	6.12	156	PSA1	96.4	27.5	0.718
41,158	6.01	49	YNL134C	14.9	1.5	0.316
41,623	7.18	58	BAT2	19.0	8.9	0.250
41,728	7.29	110	ERG10	24.1	4.5	0.543
41,900	5.42	74	TOM40	22.3	2.2	0.375
42,402	6.29	45	CYS3	6.7	8.9	0.621
42,883	5.63	67	DYS1	15.8	5.2	0.526
43,409	6.31	107	SER1	10.5	1.5	0.292
43,421	5.59	91	ERG6	2.2	14.1	0.408
44,174	7.32	56	YBR025C	13.1	6.0	0.684
44,682	4.99	72	TIF1	2.9	39.4	0.834
44,707	7.77	108	PGK1	23.7	165.7	0.897
44,707	7.77	109	PGK1	315.2	165.7	0.897
46,080	6.72	30	CAR2	15.4	NA[c]	0.495
46,383	8.52	53	IDP1	7.7	0.7	0.436
46,553	5.98	47	IDP2	32.4	NA[c]	0.197
46,679	6.39	50	ENO1	35.4	0.7	0.930
46,679	6.39	51	ENO1	6.6	0.7	0.930
46,679	6.39	52	ENO1	2.2	0.7	0.930
46,773	5.82	63	ENO2	15.5	289.1	0.960
46,773	5.82	64	ENO2	635.5	289.1	0.960
46,773	5.82	65	ENO2	93.0	289.1	0.960
46,773	5.82	66	ENO2	31.0	289.1	0.960
47,402	6.09	126	COR1	2.5	0.7	0.422
47,666	8.98	54	AAT2	11.7	6.0	0.338
48,364	5.25	73	WTM1	74.5	13.4	0.365
48,530	6.20	61	MET17	38.1	29.0	0.576
48,904	5.18	69	LYS9	16.2	3.7	0.463
48,987	4.90	153	SUP45	29.6	11.9	0.377
49,727	5.47	70	PRO2	13.6	5.2	0.297
49,912	9.27	62	TEF2	558.5	282.0	0.932
50,444	5.67	35	YDR190C	4.8	2.2	0.228
50,837	6.11	32	YEL047C	3.8	1.5	0.387
50,891	4.59	151	TUB2	11.2	7.4	0.404
51,547	6.80	27	LPD1	18.9	2.2	0.351
52,216	7.25	29	SHM2	19.7	7.4	0.722
52,859	5.54	37	YFR044C	30.2	6.7	0.442
53,798	5.19	71	HXK2	26.5	7.4	0.756
53,803	6.05	145	GYP6	4.4	0.7	0.147

TABLE 1—*Continued*

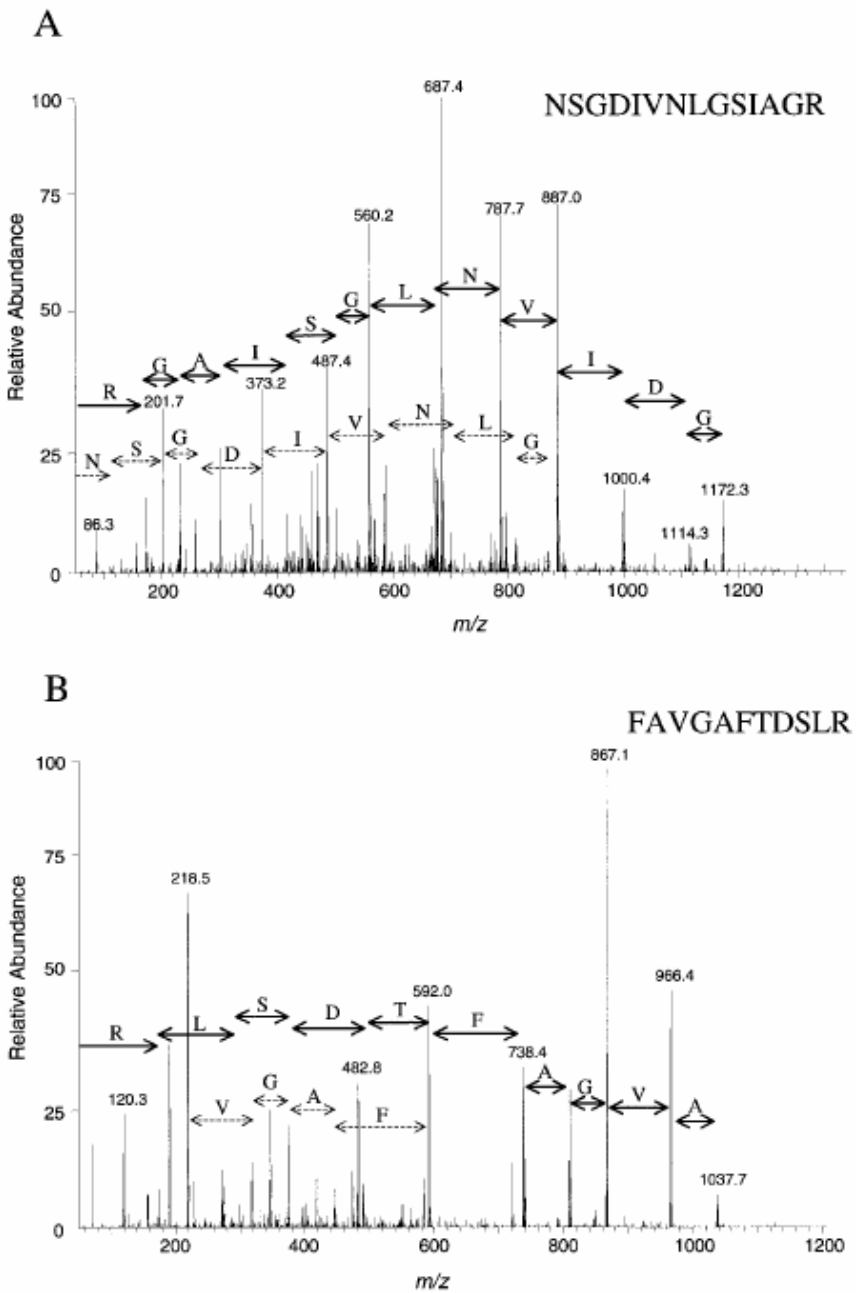

FIG. 3. Tandem mass (MS/MS) spectra resulting from analysis of a single spot on a 2D gel. The first quadrupole selected a single mass-to-charge ratio (m/z) of 687.2 (A) or 592.6 (B), while the collision cell was filled with argon gas, and a voltage which caused the peptide to undergo fragmentation by CID was applied. The third quadrupole scanned the mass range from 50 to 1,400 m/z. The computer program Sequest (8) was utilized to match MS/MS spectra to amino acid sequence by database searching. Both spectra matched peptides from the same protein, S57593 (yeast hypothetical protein YMR226C). Five other peptides from the same analysis were matched to the same protein.

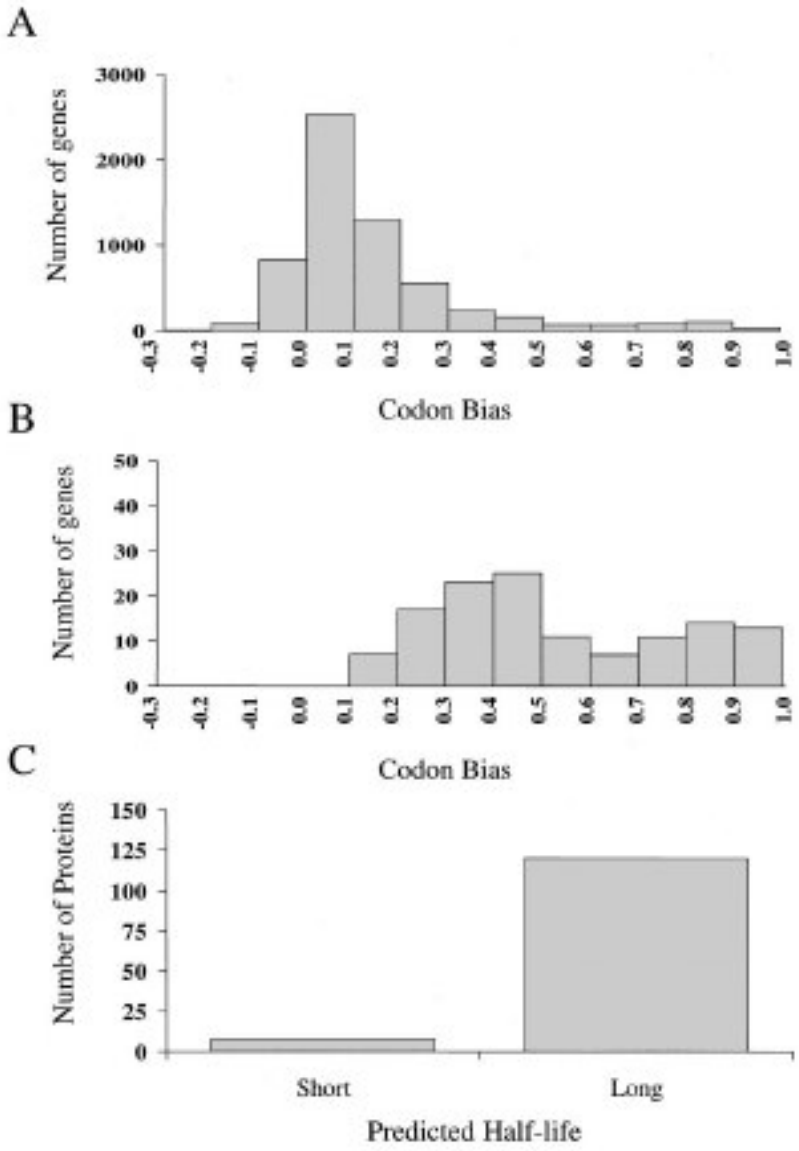

FIG. 4. Current proteome analysis technology utilizing 2DE without preenrichment samples mainly highly expressed and long-lived proteins. Genes encoding highly expressed proteins generally have large codon bias values. (A) Distribution of the yeast genome (more than 6,000 genes) based on codon bias. The interval with the largest frequency of genes is 0.0 to 0.1, with more than 2,500 genes. (B) Distribution of the genes from identified proteins in this study based on codon bias. No genes with codon bias values less than 0.1 were detected in this study. (C) Distribution of identified proteins in this study based on predicted half-life (estimated by N-end rule).

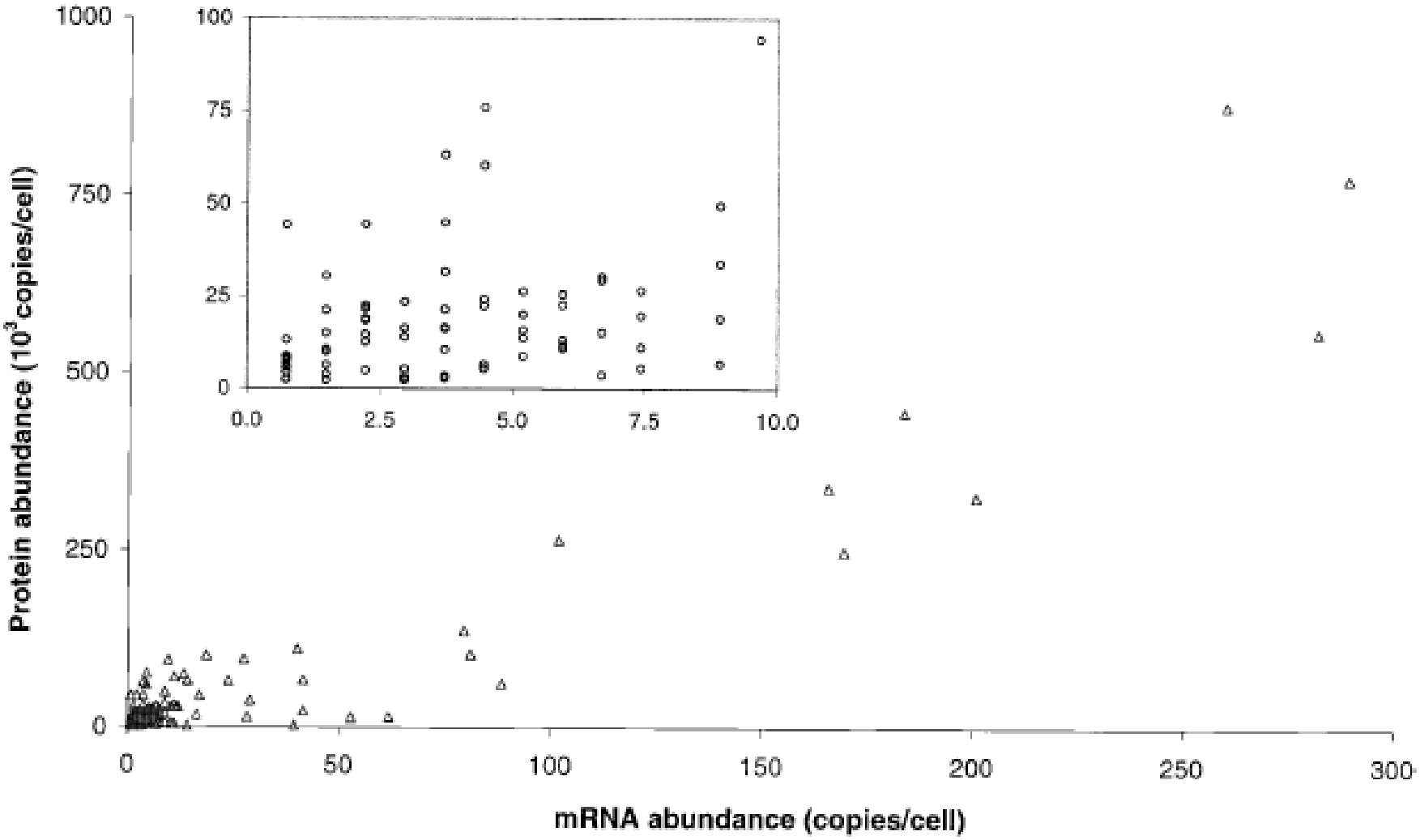

FIG. 5. Correlation between protein and mRNA levels for 106 genes in yeast growing at log phase with glucose as a carbon source. mRNA and protein levels were calculated as described in Materials and Methods. The data represent a population of genes with protein expression levels visible by silver staining on a 2D gel chosen to include the entire range of molecular weights, isoelectric focusing points, and staining intensities. The inset shows the low-end portion of the main figure. It contains 69% of the original data set. The Pearson product moment correlation for the entire data set was 0.935. The correlation for the inset containing 73 proteins (69%) was only 0.356.

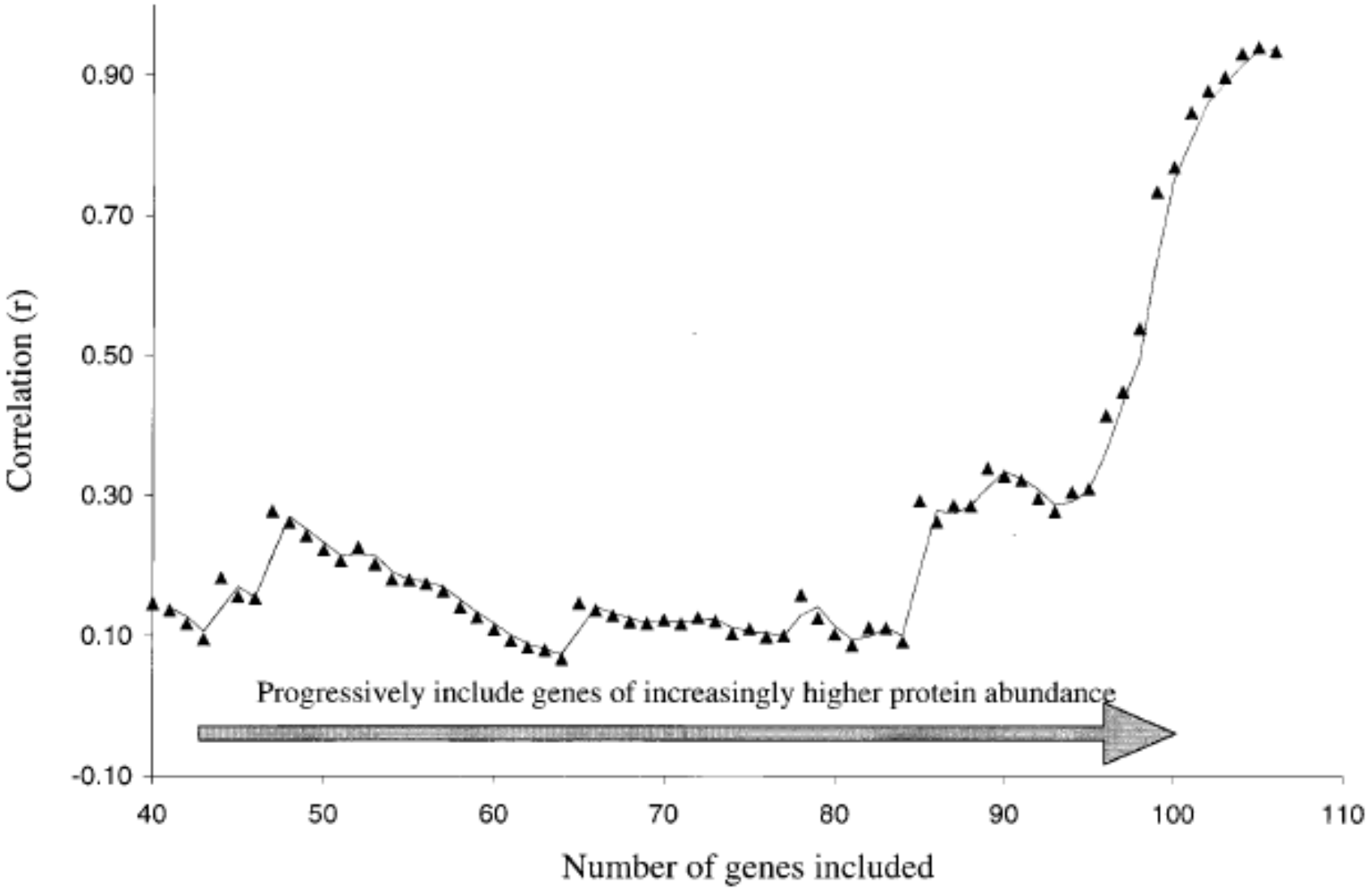

FIG. 6. Effect of highly abundant proteins on Pearson product moment correlation coefficient for mRNA and protein abundance in yeast. The set of 106 genes was ranked according to protein abundance, and the correlation value was calculated by including the 40 lowest-abundance genes and then progressively including the remaining 66 genes in order of abundance. The correlation value climbs as the final 11 highly abundant proteins are included.

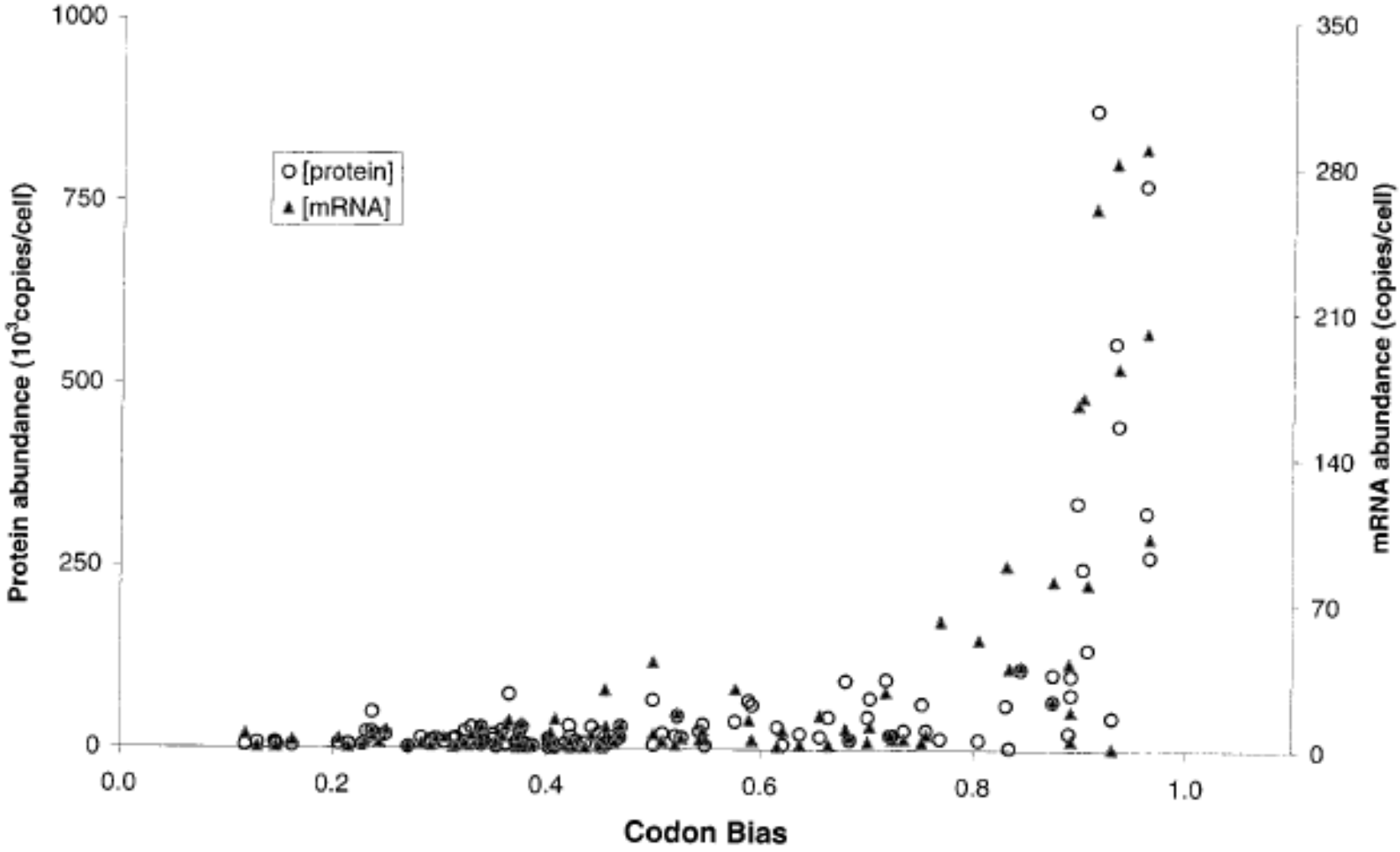

FIG. 7. Relationship between codon bias and protein and mRNA levels in this study. Yeast mRNA and protein expression levels were calculated as described in Materials and Methods. The data represent the same 106 genes as in Fig. 5.

THE JOURNAL OF BIOLOGICAL CHEMISTRY
Vol. 278, No. 9, Issue of February 28, pp. 7607–7616, 2003

Printed in U.S.A.

Global Profiling of the Cell Surface Proteome of Cancer Cells Uncovers an Abundance of Proteins with Chaperone Function*

Received for publication, October 11, 2002, and in revised form, December 13, 2002
Published, JBC Papers in Press, December 18, 2002, DOI 10.1074/jbc.M210455200

Bong Kyung Shin‡, Hong Wang‡, Anne Marie Yim‡, Francois Le Naour‡, Franck Brichory‡§, Jun Ho Jang‡, Rong Zhao‡, Eric Puravs‡, John Tra‡, Claire W. Michael¶, David E. Misek‡‖, and Samir M. Hanash‡

From the Departments of ‡Pediatrics and ¶Pathology, University of Michigan, Ann Arbor, Michigan 48109-0656

There is currently limited data available pertaining to the global characterization of the cell surface proteome. We have implemented a strategy for the comprehensive profiling and identification of surface membrane proteins. This strategy has been applied to cancer cells, including the SH-SY5Y neuroblastoma, the A549 lung adenocarcinoma, the LoVo colon adenocarcinoma, and the Sup-B15 acute lymphoblastic leukemia (B cell) cell lines and ovarian tumor cells. Surface membrane proteins of viable, intact cells were subjected to biotinylation then affinity-captured and purified on monomeric avidin columns. The biotinylated proteins were eluted from the monomeric avidin columns as intact proteins and were subsequently separated by two-dimensional PAGE, transferred to polyvinylidene difluoride membranes, and visualized by hybridization with streptavidin-horseradish peroxidase. Highly reproducible, but distinct, two-dimensional patterns consisting of several hundred biotinylated proteins were obtained for the different cell populations analyzed. Identification of a subset of biotinylated proteins among the different cell populations analyzed using matrix-assisted laser desorption ionization and tandem mass spectrometry uncovered proteins with a restricted expression pattern in some cell line(s), such as CD87 and the activin receptor type IIB. We also identified more widely expressed proteins, such as CD98, and a sushi repeat-containing protein, a member of the selectin family. Remarkably, a set of proteins identified as chaperone proteins were found to be highly abundant on the cell surface, including GRP78, GRP75, HSP70, HSP60, HSP54, HSP27, and protein disulfide isomerase. Comprehensive profiling of the cell surface proteome provides an effective approach for the identification of commonly occurring proteins as well as proteins with restricted expression patterns in this compartment.

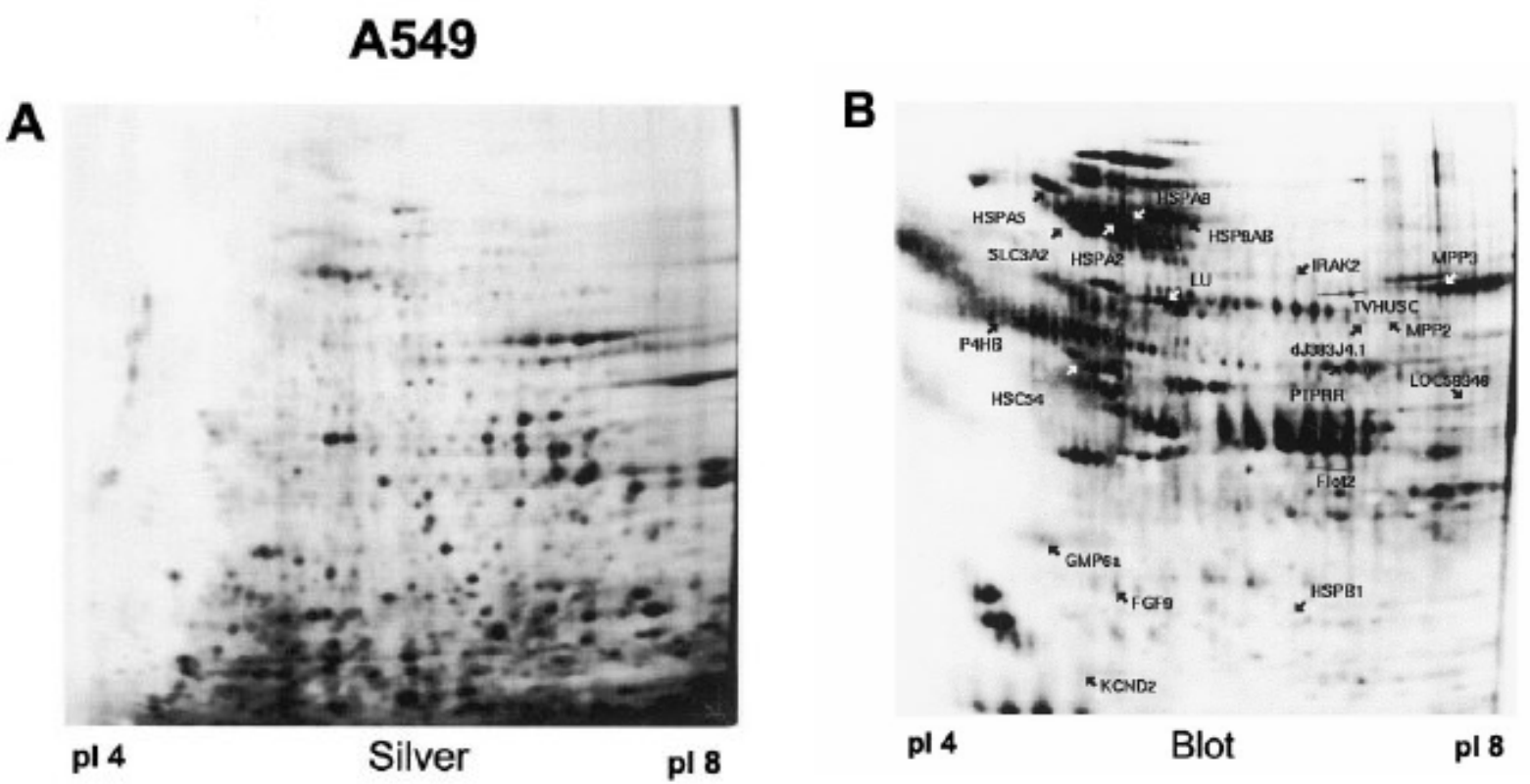

FIG. 1. **Visualization of surface biotinylation patterns in A549 lung adenocarcinoma cells.** *A*, two-dimensional PAGE analysis of cellular proteins from the A549 cell line. Solubilized proteins from A549 lung adenocarcinoma cells were resolved by two-dimensional PAGE using carrier ampholytes (pI 4–8) in the first dimension. The proteins were visualized by silver staining, as described under "Experimental Procedures." *B*, detection of biotinylated surface proteins from the A549 cell line. Intact A549 lung adenocarcinoma cells were subjected to surface biotinylation, as described under "Experimental Procedures." Solubilized proteins from the biotinylated cells were resolved by two-dimensional PAGE using carrier ampholytes (pI 4–8) in the first dimension, then transferred to PVDF membranes. The biotinylated proteins were visualized by hybridization with streptavidin-HRP complex. *Arrows* point to biotinylated proteins that were identified by mass spectrometry. Interestingly, the biotinylated proteins (*B*) are not visualized in the silver stain image of the same lysate (*A*).

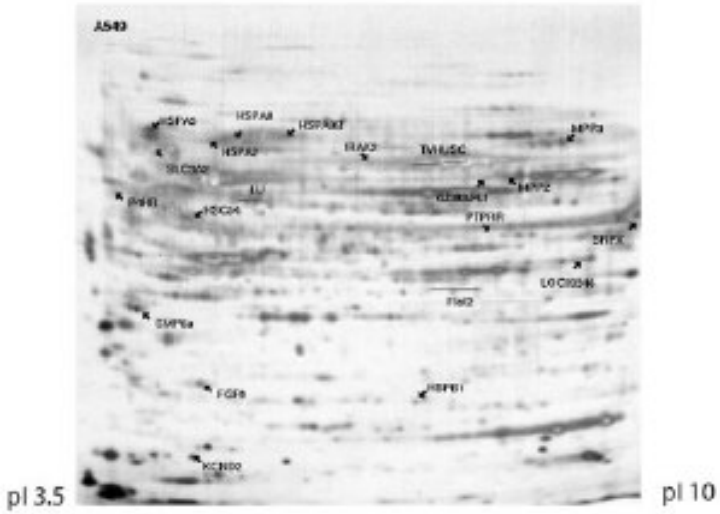

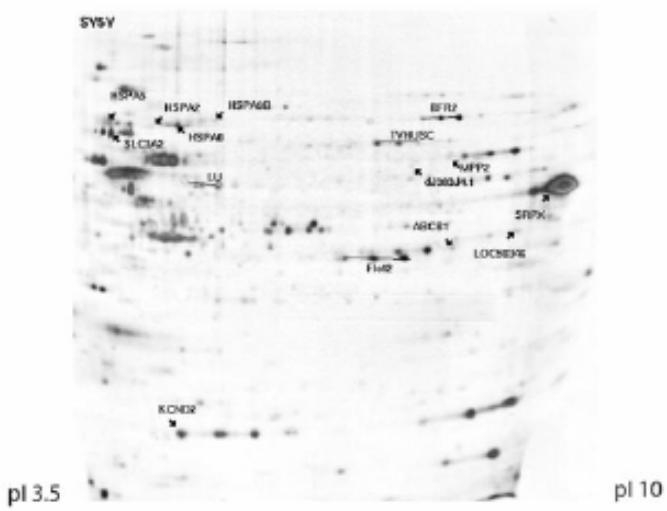

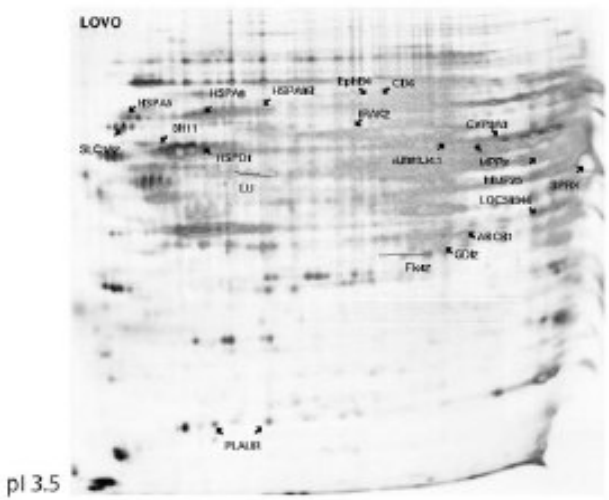

FIG. 2. **Visualization of purified biotinylated surface proteins isolated from the A549, LoVo, and SH-SY5Y cell lines.** Surface proteins of the A549, LoVo, and SH-SY5Y cell lines were biotinylated and purified as described under "Experimental Procedures." Following solubilization, the proteins were resolved by two-dimensional PAGE using IPG in the first dimension then visualized by mass spectrometry-compatible silver staining, as described under "Experimental Procedures." *Arrows* point to biotinylated proteins that were identified by mass spectrometry.

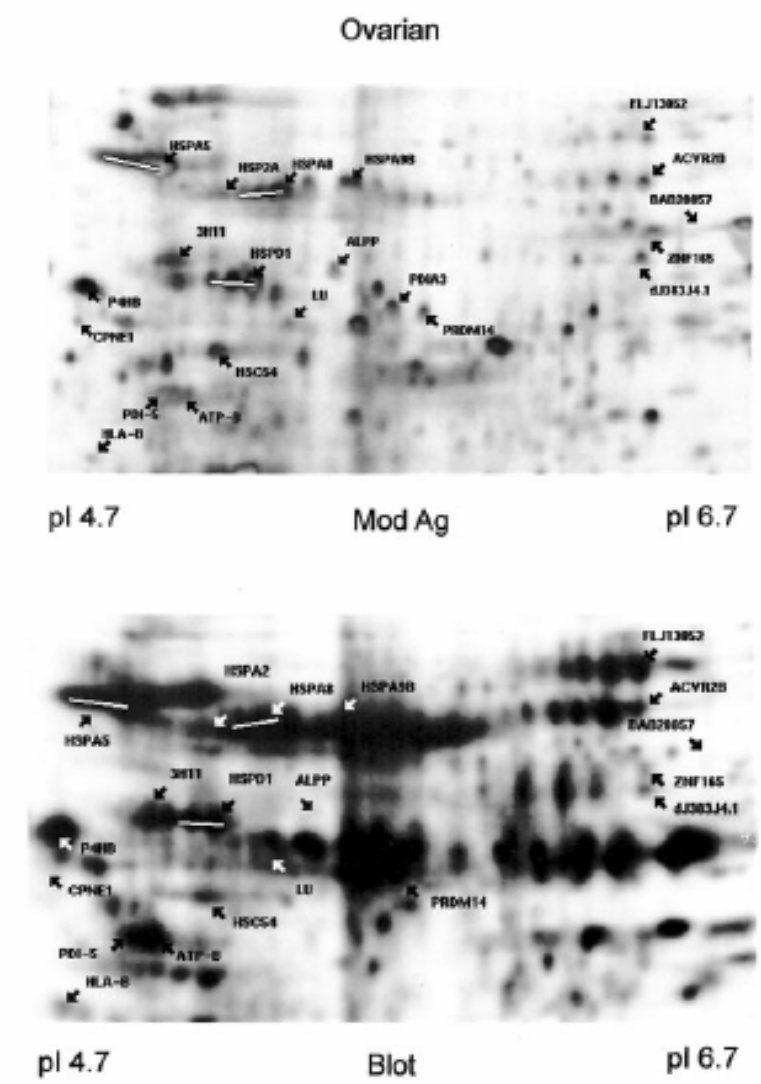

FIG. 3. **Similarity of ovarian biotinylation patterns as visualized by hybridization and silver-stained images of the same monomeric avidin column eluate.** Surface proteins of ovarian cells were biotinylated and purified as described under "Experimental Procedures." Following solubilization, the proteins were resolved by two-dimensional PAGE using carrier ampholytes (pI 4–8) in the first dimension then visualized either by mass spectrometry-compatible silver staining or hybridization with streptavidin-HRP complex, as described under "Experimental Procedures." *Arrows* point to biotinylated proteins that were identified by mass spectrometry. Interestingly, the patterns visualized by silver stain and hybridization appear to be virtually identical.

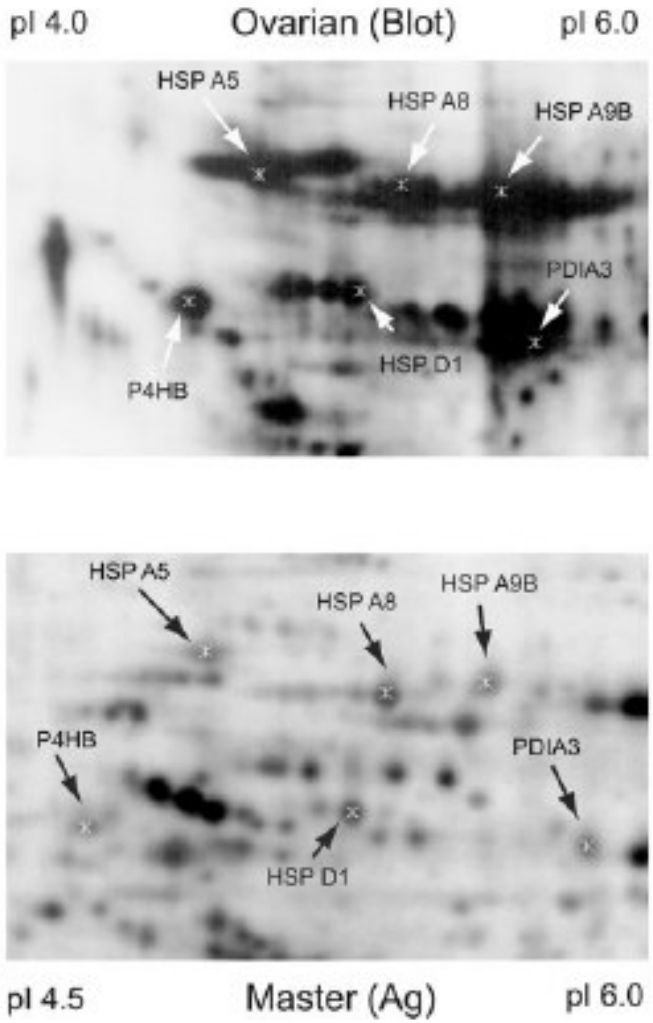

FIG. 4. **Comparison of the ovarian biotinylation patterns to a lung adenocarcinoma master image.** Surface proteins of ovarian cells were biotinylated and purified as described under "Experimental Procedures." Following solubilization, the proteins were resolved by two-dimensional PAGE using carrier ampholytes (pI 4–8) in the first dimension then visualized either by hybridization with streptavidin-HRP complex, as described under "Experimental Procedures." The image was compared with a silver stained image of a lung adenocarcinoma, which serves as a data base master image. *Arrows* point to biotinylated proteins that were found to be in common between the two images and that have been identified by mass spectrometry.

TABLE I

Identified surface proteins from the various cancer cell types

Proteins identified by cell surface biotinylation were subjected to mass spectrometry. They are indicated (MS) according to the cell type(s) that they were identified in. *Presence* or *Absence* indicates whether the protein spot was identified in other cell types by gel matching. The presence of a putative signal peptide is indicated.

	Gene symbol	Gene index number	SY5Y	A549	LoVo	Ovarian	ALL-B cell	Signal peptide
Sushi-repeat-containing protein	SRPX	gi:2498958	MS	MS	MS	Absent	Absent	Yes
Similar to PDZ-LIM Protein Mystique	LOC59346	gi:21361888	Present	MS	Present			
MAGUK P55 subfamily member 3	MPP3	gi:2497512	Absent	MS	Present			No
Lutheran blood group glycoprotein	LU	gi:1708887	MS	MS	Present	Present	Absent	No
Protein tyrosine phosphatase receptor type R	PTPRR	gi:2078323	Absent	MS		Absent	Absent	No
Voltage-sensitive potassium channel	KCND2	gi:9789986	MS	MS	Absent		Absent	Yes
4F2 antigen Heavy chain	SLC3A2	gi:177207	Present	MS	Present	Absent	Present	No
Protein-tyrosine kinase src, neuronal	TVHUSC	gi:625219	MS	MS				No
Multidrug resistance protein (P-glycoprotein)	ABCB1	gi:4505769	MS	Absent	MS	Absent	Absent	No
Rab GDP dissociation inhibitor Beta	GDI2	gi:6958323	Absent	Absent	MS			No
Cytochrome P450 nifedipine	CYP3A3	gi:510086	Absent	Absent	MS			No
MAGUK p55 subfamily member 2	MPP2	gi:2497511	Present	Present	MS	Absent	Absent	No
Interleukin-1 receptor associated kinase-2	IRAK2	gi:12230224	Absent	Present	MS		Absent	No
CD6	CD6	gi:13637684	Absent	Absent	MS			No
Ephrin type-B receptor 4	EphB4	gi:13279062	Absent	Absent	MS			No
Colon tumor antigen 3H11		gi:12711598	Absent	Absent	MS	Present	Present	No
60-kDa heat-shock protein	HSPD1	gi:129379	Present	Present	MS	MS	Present	No
u-plasminogen activator receptor form 2	PLAUR	gi:4335704		Absent	MS		Absent	Yes
Membrane type matrix metalloproteinase 6	MMP25	gi:12585274			MS			Yes
78-kDa glucose-regulated protein, BiP	HSPA5	gi:14916999	Present	Present	Present	MS	Present	No
Heat-shock 70-kDa protein 2	HSPA2	gi:1708307	Present	Present		MS	Present	No
GRP75	HSPA9B	gi:21264428	Present	Present	Present	MS	MS	No
Kelch-like protein X	dJ383J4.1	gi:12314036	Present	Present	Present	MS	Present	No
Protein disulfide isomerase	P4HB	gi:339647		Present		MS	Present	Yes
Alkaline phosphatase, placental	ALPP	gi:130738		Absent		MS	Present	Yes
Heat-shock cognate protein, 54 kDa	HSC54	gi:11526572		Present		MS	Present	No
Cation-dependent mannose-6-P receptor	M6PR	gi:106962				MS		Yes
Membrane glycoprotein M6-a	GPM6a	gi:2506889		Present		MS	Present	No
Membrane progesterone receptor component 1	PGRMC1	gi:5729875				MS	Present	No
Heat-shock 27-kDa protein 1	HSPB1	gi:4504517		Present		MS		No
Heat-shock cognate 71 kDa protein	HS7C	gi:5729877				MS		No
Activin receptor type IIB precursor	ACVR2B	gi:20532386	Absent	Absent	Absent	Present	MS	Yes
Fibroblast growth factor receptor 2	BFR2	gi:399110	MS	Absent	Absent		Absent	Yes
Flotilin 2	FLOT2	gi:13277550	MS	Present	Present	Absent	Absent	No

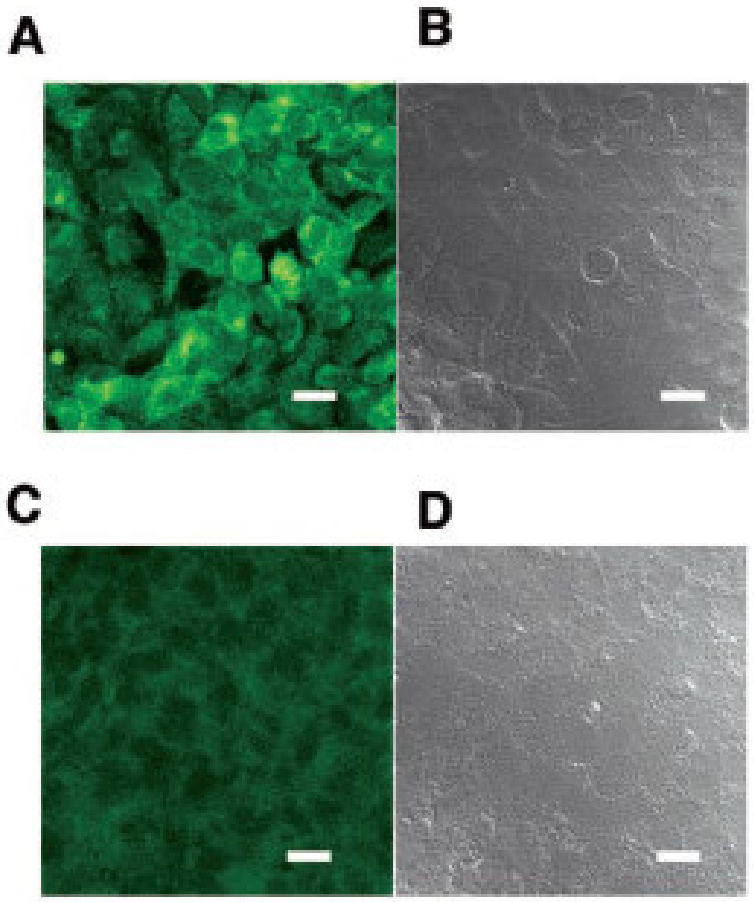

FIG. 5. **The Ephrin B4 receptor is expressed in a restricted pattern between the LoVo and A549 cell lines.** LoVo colon carcinoma and A549 lung adenocarcinoma cells were plated and grown for 48 h then fixed and stained for immunofluorescence with Rabbit anti-EphB4 antibodies, as described under "Experimental Procedures." Identical fields are shown for both the immunofluorescence and the transmitted light image (differential interference contrast). The LoVo cell line is shown in *A* and *B*. The A549 cell line is shown in *C* and *D*. *Bar*, 20 μm.

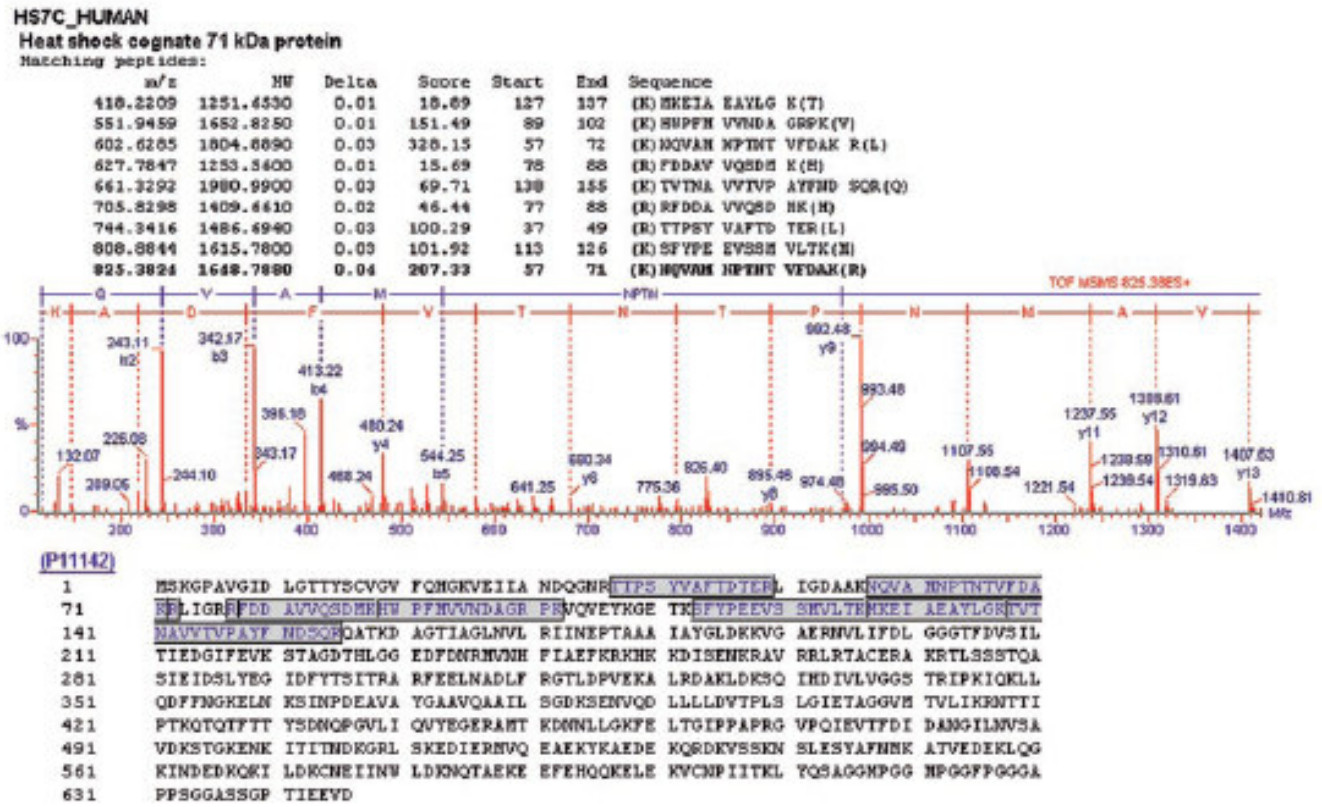

FIG. 6. **Identification of HSP71 by Q-TOF mass spectrometry.** The MS/MS spectrum of HSP71 obtained after trypsin digestion is shown by analysis with ESI-Q-TOF, coupled with nanoflow capillary high-performance liquid chromatography. The precursor ion shown in the figure is *m/z* 825.3824, and resultant peaks were searched against the non-redundant SwissProt protein sequence data base using the ProteinLynx global server. A total of nine tryptic peptides, as shown, matched the heat-shock cognate 71-kDa protein.

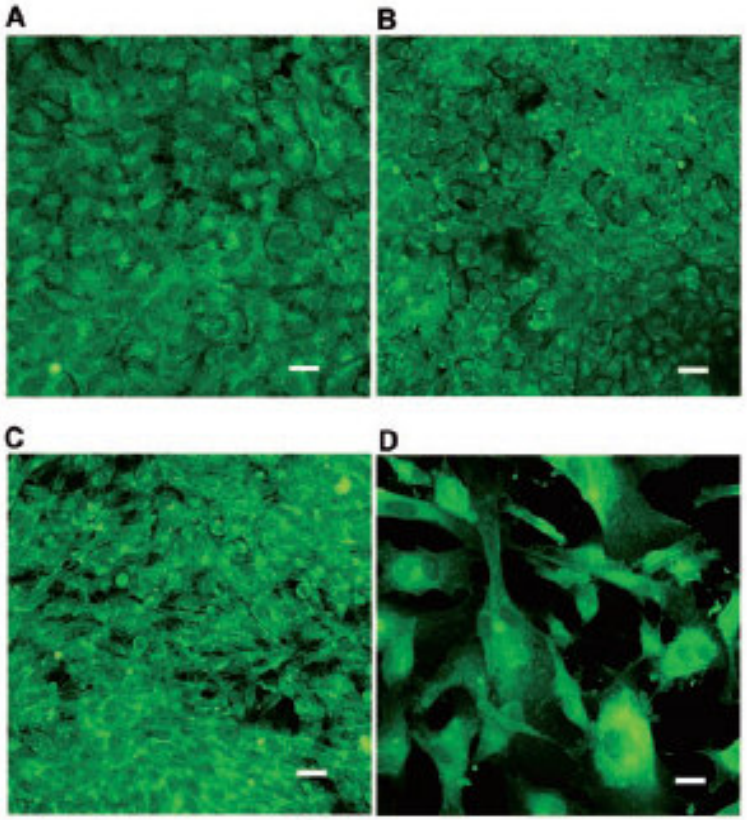

FIG. 7. **GRP78 is expressed on the cell surface in a ubiquitous pattern.** Ovarian, SH-SY5Y, LoVo, and A549 cells were plated and grown for 48 h then fixed and stained for immunofluorescence with goat anti-GRP78 antibodies, as described under "Experimental Procedures." The A549 cell line is shown in *A*, the LoVo cell line is shown in *B*, the SH-SY5Y cell line is shown in *C*, and the ovarian cells are shown in *D*. *Bar*, 20 μm.

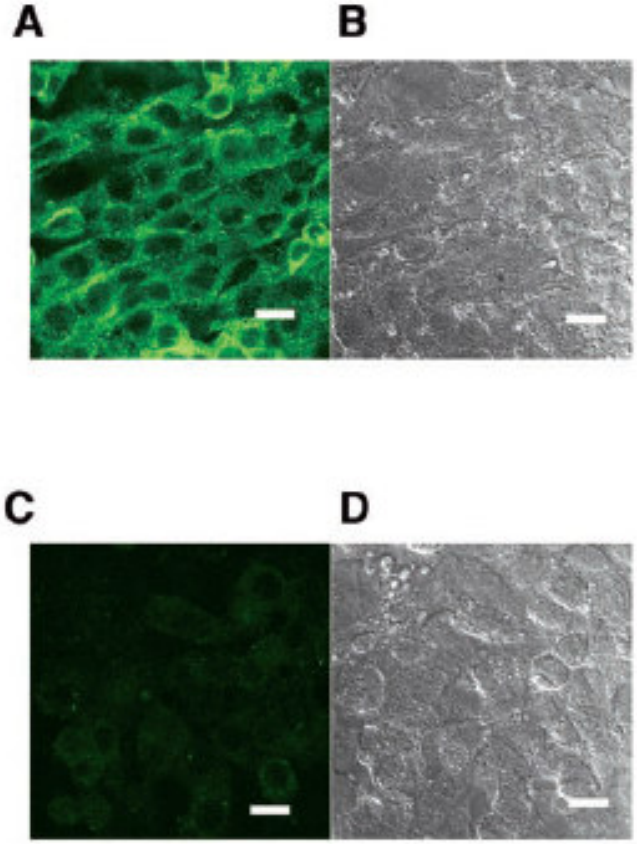

FIG. 8. **HSP70 is expressed on the cell surface of LoVo cells.** LoVo colon carcinoma cells were plated and grown for 48 h then fixed and stained for immunofluorescence with mouse anti-HSP70 antibodies, as described under "Experimental Procedures." Identical fields are shown for both the immunofluorescence and the transmitted light image (differential interference contrast). Anti-HSP70 staining is shown in *A* and *B*. The staining obtained with normal mouse IgG is shown in *C* and *D*. *Bar*, 20 μm.

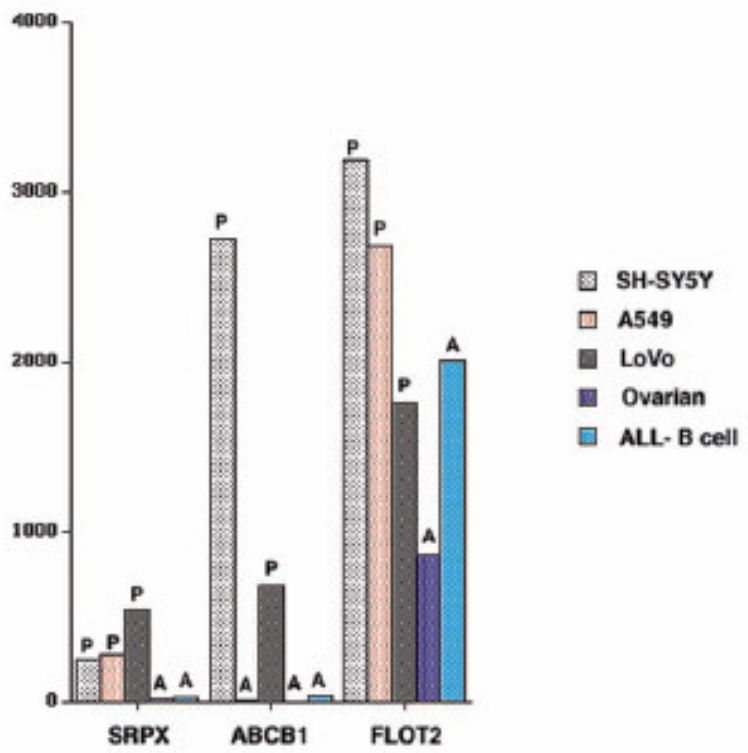

FIG. 9. **Concordance of genomic and proteomic data for SRPX, ABCB1, and FLOT2 in the various cell types examined.** mRNA expression levels were determined for SRPX, ABCB1, and FLOT2 by analysis of high density oligonucleotide microarray data, as described under "Experimental Procedures," and are shown in the graph. The presence of protein expression (*P*) or absence of protein expression (*A*) in the identified protein spot is as indicated. Interestingly, for SRPX and ABCB1 there was strict concordance between genomic and proteomic data for all cell types. For FLOT2, however, it appears by genomic data that FLOT2 is expressed ubiquitously in all of the cell types, although the protein spot of interest was absent in the ovarian and ALL-B cells.